International Journal of Modern Physics C
Vol. 34, No. 8 (2023) 2350110 (11 pages)

DOI: 10.1142/S0129183123501103

World Scientific
www.worldscientific.com

Charge transport in two-dimensional disordered systems with an external electric field

R. F. Dutra*, M. S. Santos Junior*, D. Messias*,
C. V. C. Mendes*, M. O. Sales† and F. A. B. F. de Moura*,‡

*Instituto de Física, Universidade Federal de Alagoas
Maceió, AL 57072-970, Brazil

†Instituto Federal do Maranhão (IFMA)
Campus São João dos Patos
Rua Padre Santiago, s/n, Centro
São João dos Patos, MA 65665-000, Brazil
‡fidelis@fis.ufal.br

Received 1 July 2022
Accepted 4 January 2023
Published 6 February 2023

In this paper, we consider a square lattice with correlated random hopping terms under the effect of an external electric field. We analyzed the dynamics of an initially localized electronic wave packet using a Taylor formalism to solve the Schrödinger dynamic equation. Our calculations suggest that the correlated disorder promotes a fast electronic propagation for intermediate times. When we switch on a static electric field, we observe an oscillatory behavior similar to the well-known "Bloch oscillations" phenomenology. We calculate the frequency of these oscillations, and our results are in good agreement with those predicted by the semiclassical approach used in crystalline lattices. Based on the local disorder and in the absence of extended states in our model, we discussed the stability of these apparent "Bloch oscillations".

Keywords: Localization; correlated disorder; electric field.

1. Introduction

It is known that the eigenstates are extended in a pure periodic system. The nature of an electron's eigenstates is modified when lattice imperfections generate disorders. The investigation of the dynamics of a particle in a quantum network becomes more exciting with results from Anderson's localization theory.[1–21] In 1958, Anderson showed in his paper that disordered solids have localized electronic states for a range of energy.[4] It was demonstrated that in one-dimensional and two-dimensional systems, for any degree of uncorrelated disorder, the electronic states are exponentially localized.[4,8] Localized and delocalized states can coexist in different energy ranges for

‡Corresponding author.

three-dimensional systems. But when dealing with low-dimensional systems, in which the disorder distribution presents intrinsic correlations, the eigenstates can be delocalized. That is, the disorder correlation can create extended states for some energy values.[22–28] These studies aroused attention in investigating the existence of a metal–insulator transition in low-dimensional systems that contain the correlated disorder.

One of the successful works considers a variant of the Anderson model with the correlated disorder in the dimers distribution.[23] For this model, the chain contains hopping terms equal to t and two types of atoms with energies ϵ_1 and ϵ_2 (in units of t). The results showed that there are extended states whenever one of the sites' energies appears in pairs. In Ref. 24, the possibility of mapping polyaniline to a random dimer model was demonstrated. Furthermore, experimental investigations of the effects of these dimer correlations on a GaAs–AlGaAs (SL) superlattice revealed the emergence of extended states.[25] References 26 and 27 theoretically demonstrated the emergence of a band of extended state in the Anderson model with long-range correlations without a characteristic length scale. Furthermore, experimental investigations, such as those performed on rectangular waveguides of microwave transmission, helped prove the existence of extended states in low-dimensional systems with scale-free correlated disorder.[28] Some stochastic processes in nature, such as the nucleotide sequence of DNA molecules, are known to generate long-range, free-scale, correlated random sequences.[29,31] References 30 and 31 pointed out the importance of long-range underlying correlations for electronic transport in DNA. In Ref. 31 was considered a one-dimensional Anderson model with long-range correlated disorder distribution in hopping and on-site energies. The model assumes a binary alloy with its nearest on-site and hopping energies mapped to two values. The results showed that the localization length increases when the intrinsic correlations also increase.

Anderson's localization model of noninteracting atomic gases in disordered optical lattices describes the effect of a simple cubic optical lattice with a superimposed isotropic blue-detuned optical speckle field.[32] The results showed a dependence on the intensity of critical disorder, where the entire band becomes localized, with the localization length.[32] In Ref. 33, the phase diagram for the disorder-correlated Hubbard model at half-filling in one-dimensional is investigated. The model, without the disorder, presents a metallic phase and an insulating Mott phase. According to the Anderson model, the metallic phase becomes unstable and localizes when an arbitrarily low degree of disorder is introduced. The identification and characterization of these phases make the model attractive for optical networks and cold atoms investigations. It was observed in Ref. 34, which considers a model of a one-dimensional conductor with the correlated disorder, the appearance of extended states, and a nonzero Landauer resistance in the limit of infinite size contrary to the predictions of scale theory of Anderson's localization. Also discussed is a possible construction of a delocalization structure by stacking films and a one-dimensional photonic crystal to build a narrow-band light filter.

In Ref. 39, the interaction between Anderson localization and nonlinear effects was studied. Through a nonlinear transmission line carried out in the Toda lattice, randomness is inserted in the inductance of the transmission line. Then, the stress propagation dynamics are investigated. It was observed that voltage propagation depends on the disorder and verifies that it promotes Anderson localization when the disorder is sufficiently strong. It was also noted that nonlinearity increases localization. Experimental studies on *Cu* films have revealed the first evidence of charge transport involving weak Anderson localization.[40] Furthermore, the results verified that the localization phenomenon, expected by the quantum theory of resistivity of nanometric metallic connectors, occurs when the electrons cross several consecutive disordered grains. It was observed for the first time Anderson transverse localization in an optical fiber with a random transverse refractive index profile. This phenomenology promoted the emergence of a new class of unconventional optical fibers that guide light, using Anderson localization, in which light can guide anywhere via the random cross profile.[41] This type of fiber is used to transport high-quality endoscopic images quite successfully.

Our work investigates the electronic dynamics in a square lattice with correlated random hopping terms and under the effect of an external electric field. We analyzed the dynamics of an initial Gaussian electronic wave packet using a Taylor formalism to solve the Schrödinger dynamic equation. In the absence of an electric field, our results suggest that the correlated disorder can promote a fast electronic propagation for intermediate times. We analyze the effect of a static electric field and observe the existence of an oscillatory behavior with a frequency equal to field intensity (i.e. the same framework of the Bloch oscillations theory). We investigate the oscillations stability in light of the nature of the eigenstates and the topology of the hopping distribution.

2. Model and Formalism

We consider a one-electron moving in an $N \times N$ disordered lattice. We can write the Hamiltonian of our model as

$$H = \sum_{n,m} \epsilon_{n,m} |n,m\rangle\langle n,m| + \sum_{\langle n,m\rangle} (T_{n,m}|n,m\rangle\langle n,m+1| + Z_{n,m}|n,m\rangle\langle n+1,m|), \tag{1}$$

where $|n,m\rangle$ is a Wannier state localized at site (n,m). In our work, there is an electric field given by $\mathbf{E} = E_x\mathbf{x} + E_y\mathbf{y}$. Therefore, the on-site energy $\epsilon_{n,m}$ is given by $\epsilon_{n,m} = E_x(n - N/2) + E_y(m - N/2)$ (here we considered, $e = a = 1$[35]). $T_{n,m}$ and $Z_{n,m}$ represents the longitudinal and transversal hopping terms, respectively. The complete distribution of hopping terms (i.e. $N \times 2N$ terms) will be generated following a correlated profile $(u_{i,j})$ as follows:

$$u_{i,j} = \sum_{k,o} \frac{X_{k,o}}{(d_{ij,ko}/A + 1)^2}, \tag{2}$$

where $X_{k,o}$ are $N \times 2N$ random numbers uniformly distributed on interval $[-0.5, 0.5]$. The quantity $d_{ij,ko}$ is given by $d_{ij,ko} = \sqrt{(i-k)^2 + (j-o)^2}$ and $0 < A \leq N$ is a parameter that controls the degree of correlation within the profile $u_{i,j}$. In our model, the hopping energies are given by $T_{n,m} = 0.5\tanh(u_{n,2m}) + 1$ and $Z_{n,m} = 0.5\tanh(u_{n,2m-1}) + 1$. We emphasize that this transformation is a numerical trick that provides correlated random numbers in the off-diagonal distribution without any null hopping terms. In Figs. 1(a)–1(d), we plot the complete hopping distribution $h_{i,j} = 0.5\tanh(u_{i,j}) + 1$ at the $s(i,j)$ plane. We observe that for $A = 1$,

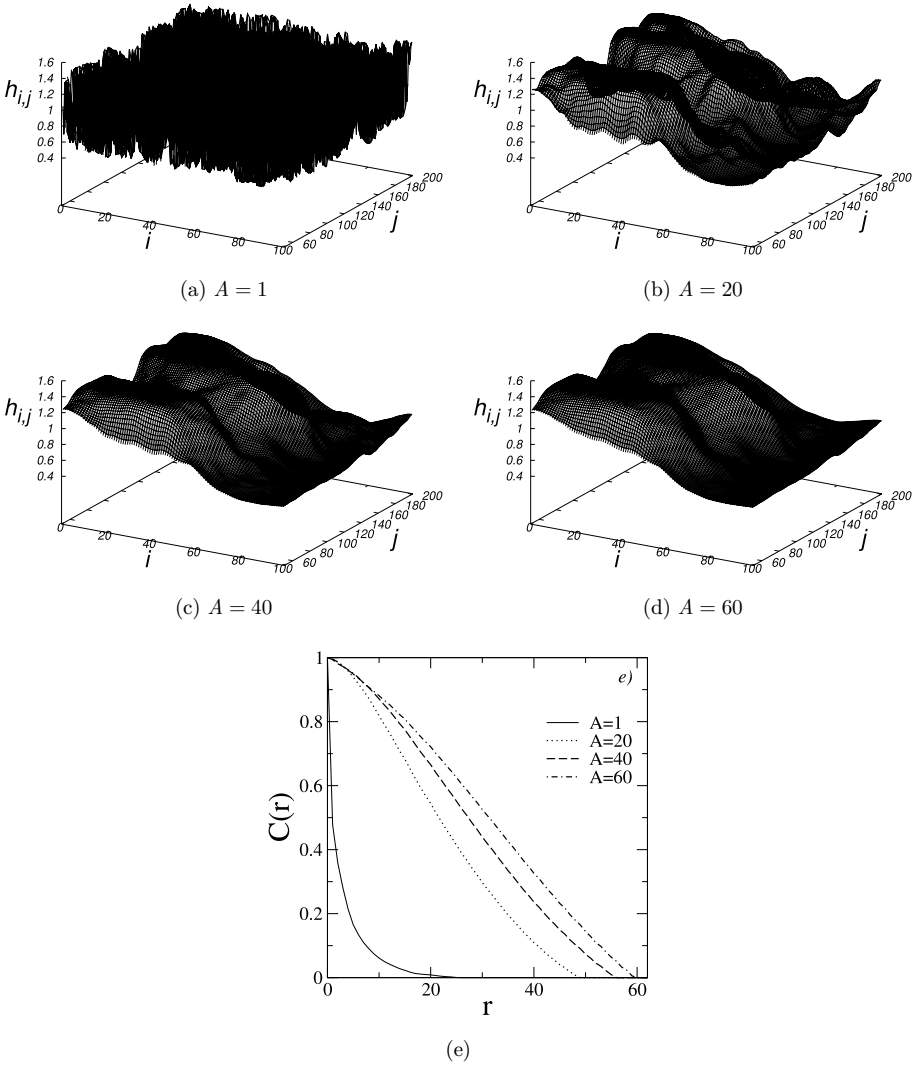

Fig. 1. (a)–(d) The complete hopping profile $h_{i,j} = 0.5\tanh(u_{i,j}) + 1$ vs i and j for $A = 1$ up to 60. (e) The auto-correlation function $C(r)$ vs r for the data found in (a)–(d).

the hopping exhibits a rough profile, while for $A = 20, 40, 60$, we can note a smoothing of the hopping distribution. In Fig. 1(e), we plot the intrinsic correlation function within the hopping distribution. We emphasize that $C(r) = [\langle h_{i,j}h_{k,o}\rangle - \langle h_{i,j}\rangle\langle h_{k,o}\rangle]/[\langle h_{i,j}^2\rangle - \langle h_{i,j}\rangle\langle h_{k,o}\rangle]$, where $r = \sqrt{(i-k)^2 + (j-o)^2}$. As the value of A is increased, the size of the correlated region also increases.

The Wannier amplitudes evolve in time according to the time-dependent Schrödinger equation as ($\hbar = 1$)[35,36]

$$\begin{aligned} i\frac{dc_{n,m}(t)}{dt} &= [E_x(n - N/2) + E_y(m - N/2)]c_{n,m} + T_{n,m-1}c_{n,m-1}(t) \\ &\quad + T_{n,m}c_{n,m+1}(t) + Z_{n-1,m}c_{n-1,m}(t) + Z_{n,m}c_{n+1,m}(t), \\ &\quad i, m = 1, 2, \ldots, N. \end{aligned} \tag{3}$$

In our calculations, we defined the initial state as a Gaussian packet with $c_{n,m}(t = 0) = (1/\Pi)\exp(-K(n,m)/4)$, where $K(n,m) = [(n - N/2)^2 + (m - N/2)^2]$ and Π is a normalization constant. The above set of equations was solved numerically by using a high-order method based on the Taylor expansion[38] of the evolution operator $U(\Delta t) = \exp(-iH\Delta t) = 1 + \sum_{l=1}^{z_o}[(-iH\Delta t)^l]/l!$ where H is the Hamiltonian. The wave function at time Δt is given by $|\Phi(\Delta t)\rangle = U(\Delta t)|\Phi(t = 0)\rangle$. We can use this method recursively to obtain the wave function at time t.

The results without electric field can be taken adopting $\Delta t = 0.1$ and the sum was truncated at $z_o = 10$. This cutoff was sufficient to keep the considered wave function norm conservation along the entire time interval. In the case of considering an electric field, we have used $\Delta t = 0.01$ and $z_0 = 12$. In the absence of an electric field, we will investigate the participation number defined as

$$P(t) = 1 \Bigg/ \left[\sum_{n=1}^{N}\sum_{m=1}^{N}|c_{n,m}(t)|^4\right]. \tag{4}$$

Note that $P(t)$ varies from 1, for a wave function confined to a single site, to N^2, for a wave uniformly extended over the whole lattice.[35–37] In addition, we also will investigate the temporal auto-correlation function $\Theta(t)$ defined as

$$\Theta(t) = \frac{1}{t}\int_0^t J(t)dt, \tag{5}$$

where $J(t) = \sum_{i,j}[c_{i,j}(t = 0)c_{i,j}(t)]$ works as a generalized return probability. For localized states, the temporal auto-correlation function $\Theta(t)$ is roughly a constant. For extended states $\Theta(t) \propto 1/t$. In the presence of an external electric field, we will analyze the electronic mean position defined as

$$R(t) = \frac{1}{\sqrt{2}}(\mathbf{x} + \mathbf{y}) \cdot (\langle n\rangle(t)\mathbf{x} + \langle m\rangle(t)\mathbf{y}), \tag{6}$$

where $\langle n\rangle(t) = \sum_{n=1}^{N}\sum_{m=1}^{N} n|c_{n,m}(t)|^2$ and $\langle m\rangle(t) = \sum_{n=1}^{N}\sum_{m=1}^{N} m|c_{n,m}(t)|^2$.

3. Results

We show our results without an electric field (i.e. $E_x = E_y = E = 0$). We solve the complete Schrödinger equation considering $N = 300$ up to 1200. We emphasize that, for initial times, we did not solve the set of equations for all $N \times N$ sites. We considered a finite fraction of size $L_0 \times L_0$ around the lattice center. Then, we monitored the wave packet at the borders of this small region and expanded L_0 until it reached $L_0 = N$. It is a numerical trick to speed up the calculations. We have used about 100 distinct disorder realizations to compute all quantities. In Fig. 2, we plot the re-scaled long-time participation number defined as $P_\infty/N^2 = P(t \to t_{\max})/N^2$. This quantity is roughly a constant independent of N, for extended states.

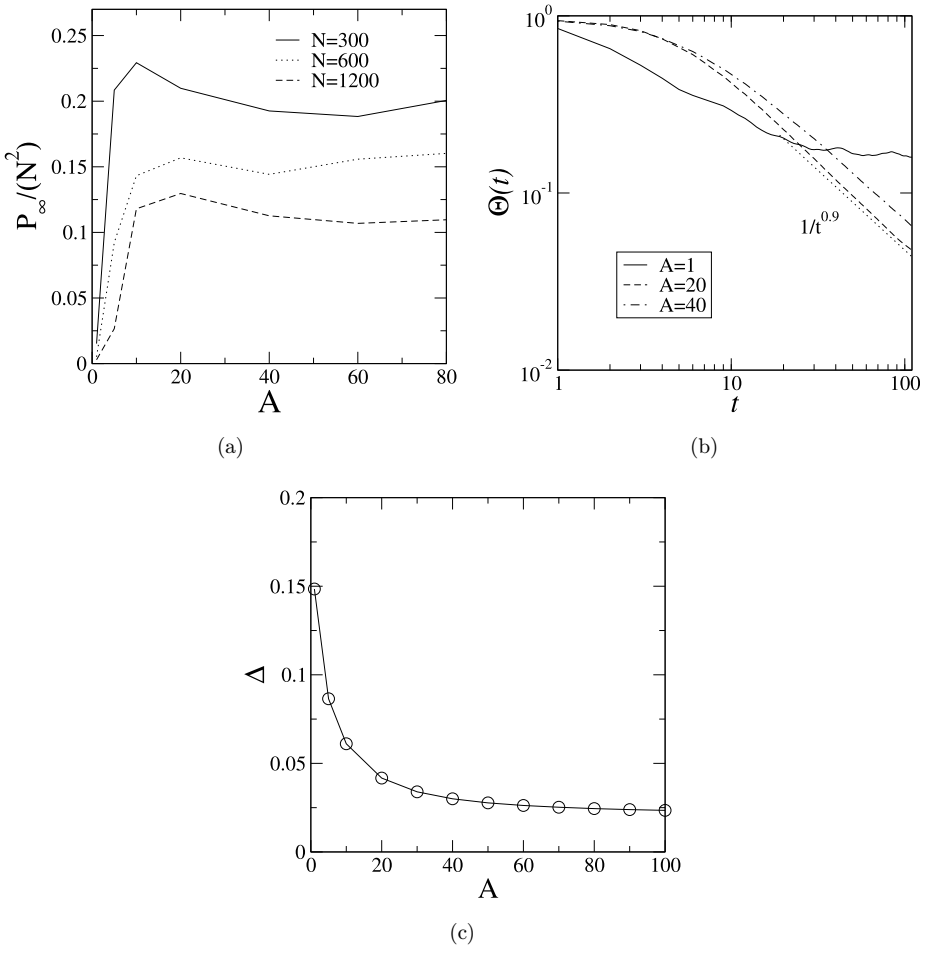

Fig. 2. (a) The re-scaled long-time participation number $P_\infty/N^2 = P(t \to \infty)/N^2$ vs A for $N = 300$ up to 1200. (b) The temporal auto-correlation function $\Theta(t)$ vs t for $A = 1, 20, 40$. (c) The local variance Δ of the hopping distribution. Calculations of Δ were done using $N = 100$, $x_0 = 10$ and $N_c = 200$ and about 100 distinct disorder realizations. The local disorder decreases as the value of A are increased.

For localized states, P_∞/N^2 goes to zero as the system size increases. For all cases considered here in the absence of electric field, we have used $t_{\max} \approx 2N$. We can see that the re-scaled long-time participation number P_∞/N^2 goes to zero as the N is increased. It is a clear signature of localized states at the thermodynamic limit. We stress that the participation seems larger for $A > 1$. Therefore, our results suggest that the participation number becomes bigger as the A increases. We emphasize that P_∞ does not scale proportional to the area N^2; however, its big values indeed suggest that some eigenstates contain great localization lengths (for $A \gg 1$). The temporal auto-correlation function $\Theta(t)$ (see Fig. 2(b)) also exhibits a nonusual behavior. The temporal auto-correlation for small A is roughly a constant, thus suggesting localized states. However, for $A = 20, 40$, we observe that the $\Theta(t)$ exhibits vanishing as $1/t^{0.9}$. This result suggests that the generalized return probability ($J(t)$) exhibits some decrease with time (at least within that time scale we are enabled to consider). This phenomenology is possibly related to the local topology of the hopping distribution. To understand better this key point, we calculate the local variance Δ of the hopping distribution. We divide the hopping profile $h_{i,j}$ in cells of size $x_0 \times x_0$. We calculate the local variance Δ_m within each cell (here m runs over all cells). The quantity Δ is defined as $\Delta = \sum_m \Delta_m/N_c$ where N_c is the number of cells. In our calculations of Δ, we consider $N = 100$, $x_0 = 10$ and $N_c = 200$ and about 100 distinct disorder realizations. The plot of Δ vs A can be found in Fig. 2(c). We can see that as the value of A increases, the quantity Δ decreases. Therefore, as the degree of correlations increases, the hopping distribution's local disorder becomes weak. We emphasize that this effect is related to the smoothing of the hopping profile observed in Figs. 1(a)–1(d). Therefore, our results suggest that extended states are absent within our model. However, our calculations of participation number and auto-correlation function also indicate the presence of states with great localization lengths. The correlated sequence considered here contains a weak local disorder that promotes the appearance of weakly localized modes. In some cases, these states with great localization lengths may actually be critical states.

In the presence of a static electric field parallel to the lattice (i.e. $\mathbf{E} = E_x\mathbf{x} + E_y\mathbf{y}$ with $E_x = E_y = E$) our results can be summarized in Figs. 3–6. We initially emphasize that in crystalline lattices, a static electric field promotes the appearance of oscillatory dynamics (also called "Bloch oscillations") with frequency $\omega_E = E$. Moreover, the region's size in the wave packet remains trapped increases as the electric field is decreased.[38] In Figs. 3 and 4, we obtain more or less this behavior for the cases $A = 20, 40$. We observe that the wave packet remains trapped around the initial position and exhibits oscillatory dynamics with a frequency of roughly $\omega = E$. For $A = 1$, the almost uncorrelated disordered potential dampens the oscillatory dynamics, and the coherent dynamics with a single frequency are absent. Therefore, our results for $A = 20, 40$ indicate that a "Bloch's like oscillations" is induced by this correlated disorder. However, it is necessary to be careful with the data to conclude the analysis. We stress that even for $A \approx N$ the extended states are absent. For $A \gg 1$, our previous calculations demonstrate that this model contains states with

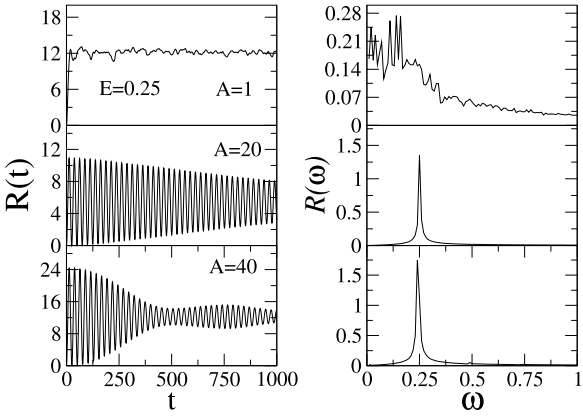

Fig. 3. The mean position $R(t)$ vs t for $A = 1, 20, 40$ and its Fourier transform $R(\omega)$ for $E = 0.25$. We observe that the wave packet remains trapped around the initial position and exhibits oscillatory dynamics with a frequency of roughly $\omega = E$. For $A = 1$, we observe that the weak correlated disordered potential dampens the oscillatory dynamics, and the coherent dynamics with a single frequency are absent.

big localization lengths but still localized states. We also show that the local disorder decreases as the value of A increases. Therefore, the results obtained in Figs. 3 and 4 do not represent stable Bloch's oscillations. The phenomenology obtained in Figs. 3 and 4 is valid only for initial times. For a long time, the disorder (even being locally weak) will be dumping the oscillatory dynamics and promoting a dynamics localization without coherence. In Figs. 3 and 4, it is not so easy to observe this key point due to the intensity of the electric field. For an intense electric field, the region's size where the wave packet is oscillating decreases, and therefore the effect of disorder is small (and the time to destruction of oscillation increases a lot). The analysis of the region in which the electron remains trapped can be found in Fig. 5. We plot the

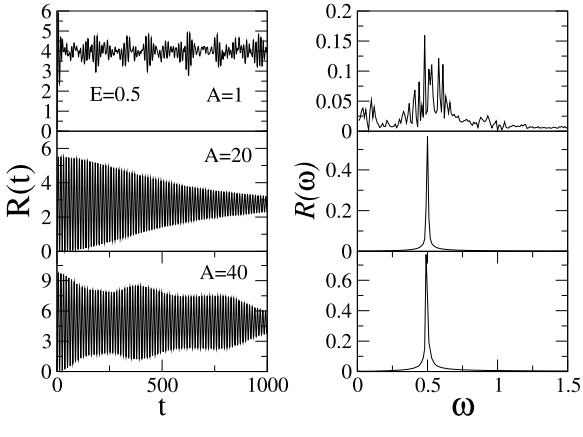

Fig. 4. The mean position $R(t)$ vs t for $A = 1, 20, 40$ and its Fourier transform $R(\omega)$ for $E = 0.5$. Similarly to the results obtained in Fig. 3, the oscillatory dynamics here $(A > 1)$ have frequency of roughly $\omega = E = 0.5$.

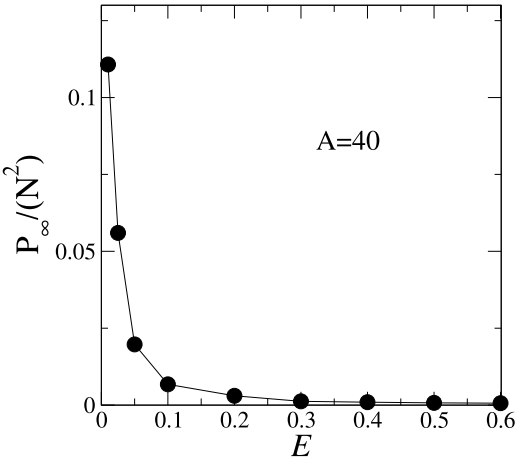

Fig. 5. The re-scaled long-time participation number $P_\infty/N^2 = P(t \to \infty)/N^2$ vs E for $N = 1200$ and $A = 40$.

normalized participation number $P_\infty/N^2 = P(t \to t_{\max})/N^2$ vs E considering a lattice with $N = 1200$ and $A = 40$. We can see clearly that the electron remains localized in a tiny region with few sites for a strong electric field. By another side, the electron can move in a large region for a weak electric field. Therefore, for a more weak field (e.g. $E = 0.1$) (see Fig. 6), we can see the duping of the oscillatory phenomenology more clearly. For a long time, the disorder promotes decreasing the oscillatory picture, and the dynamics converge to a standard dynamics localization.

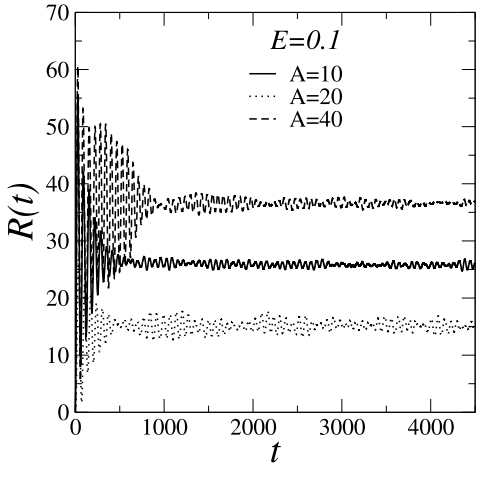

Fig. 6. The mean position $R(t)$ vs t for $E = 0.1$ and $A = 1, 20, 40$. For a long time, the disorder promotes the decreasing of the oscillatory picture, and the dynamics converge for a standard dynamics localization.

4. Conclusion

In summary, we investigate the dynamics of a wave packet initially located in a square lattice with correlated hopping terms. Using Taylor's method, we find the solutions to Schrödinger's dynamic equation. The results show a clear signature of localized states in the absence of an electric field. Furthermore, the participation number and auto-correlation function calculations indicated the presence of states with great localization lengths. Using numerical analysis of the disorder distribution, we have shown that the appearance of these states with big localization lengths is related to the smoothing of the local disorder. When a static electric field is inserted in the system, an oscillatory behavior similar to the "Bloch oscillations" is induced by this type of correlated disorder for an intermediate time interval. We also calculated the frequencies of these oscillations and showed that they agree with the results predicted by the semi-classical approach. We emphasize that the disorder promotes a decrease in the amplitude of this oscillatory picture at the long-time limit. Consequently, the dynamics converge to a standard dynamics localization. We have numerically shown that this correlated disorder in systems with $d = 2$ cannot promote the appearance of extended states or stable Bloch oscillations (at a long-time limit). The main point behind this phenomenology is the existence of a typical effective correlation length (the quantity A) within the disorder distribution. As the effective correlation length within the disorder distribution increases the localization length also increases; however, this aspect is not enough to stabilize extended states. We hope our work further stimulates the investigation of electron propagations in low-dimensional systems with correlated disorder and electric fields.

Acknowledgment

This work is supported by CNPq, CAPES, FINEP (Federal Brazilian Agencies) and FAPEAL (Alagoas State Agency).

References

1. F. M. Izrailev, A. A. Krokhin and N. M. Makarov, *Phys. Rep.* **512**, 125 (2012).
2. F. Evers and A. D. Mirlin, *Rev. Mod. Phys.* **80**, 1355 (2008).
3. D. Rivas, A. Szameit and R. A. Vicencio, *Sci. Rep.* **10**, 1 (2020).
4. P. W. Anderson, *Phys. Rev.* **109**, 1492 (1958).
5. P. A. Lee and T. V. Ramakrishnan, *Rev. Mod. Phys.* **57**, 287 (1985).
6. P. A. Lee and D. S. Fisher, *Phys. Rev. Lett.* **47**, 882 (1981).
7. B. Kramer and A. MacKinnon, *Rep. Prog. Phys.* **56**, 1469 (1993).
8. E. Abrahams, P. W. Anderson, D. C. Licciardello and T. V. Ramakrishnan, *Phys. Rev. Lett.* **42**, 673 (1979).
9. F. A. B. F. de Moura and F. Dominguez-Adame, *Eur. Phys. J. B* **66**, 165 (2012).
10. D. H. White *et al.*, *Nat. Commun.* **11**, 4942 (2020).
11. M. O. Sales and F. A. B. F. de Moura, *Physica E* **45**, 97 (2012).
12. R. N. Bhatt and S. Kettemann, *Ann. Phys.* **435**, 168664 (2021).
13. S. S. Albuquerque, F. A. B. F. de Moura and M. L. Lyra, *Physica A* **357**, 165 (2005).

14. F. A. B. F. de Moura, L. P. Viana and A. C. Frery, *Phys. Rev. B* **73**, 212302 (2006).
15. F. A. B. F. de Moura and F. Domínguez-Adame, *Eur. Phys. J. B* **66**, 165 (2008).
16. F. A. B. F. de Moura, *J. Phys., Condens. Matter* **22**, 435401 (2010).
17. M. O. Sales, T. F. Assunção, S. S. Albuquerque and F. A. B. F. de Moura, *Int. J. Mod. Phys. C* **25**, 1350091 (2014).
18. L. D. da Silva, J. L. L. dos Santos, A. Ranciaro Neto, M. O. Sales and F. A. B. F. de Moura, *Int. J. Mod. Phys. C* **28**, 1750100 (2017).
19. P. A. Morais, J. S. Andrade Jr., E. M. Nascimento and M. L. Lyra, *Phys. Rev. E* **84**, 041110 (2011).
20. M. Filoche and S. Mayboroda, *Proc. Natl. Acad. Sci. USA* **109**, 14761 (2012).
21. C. I. N. Sampaio Filho, A. A. Moreira, N. A. M. Araújo, J. S. Andrade Jr. and H. J. Herrmann, *Phys. Rev. Lett.* **117**, 275702 (2016).
22. J. C. Flores, *J. Phys., Condens. Matter* **1**, 8471 (1989).
23. D. H. Dunlap, H. L. Wu and P. W. Phillips, *Phys. Rev. Lett.* **65**, 88 (1990); H.-L. Wu and P. Phillips, *Phys. Rev. Lett.* **66**, 1366 (1991).
24. P. W. Phillips and H. L. Wu, *Science* **252**, 1805 (1991).
25. V. Bellani, E. Diez, R. Hey, L. Toni, L. Tarricone, G. B. Parravicini, F. Domínguez-Adame and R. Gómez-Alcalá, *Phys. Rev. Lett.* **82**, 2159 (1999).
26. F. A. B. F. de Moura and M. L. Lyra, *Phys. Rev. Lett.* **81**, 3735 (1998).
27. F. M. Izrailev and A. A. Krokhin, *Phys. Rev. Lett.* **82**, 4062 (1999); F. M. Izrailev, A. A. Krokhin and S. E. Ulloa, *Phys. Rev. B* **63**, 41102 (2001).
28. U. Kuhl, F. M. Izrailev, A. Krokhin and H. J. Stöckmann, *Appl. Phys. Lett.* **77**, 633 (2000).
29. C. K. Peng, S. V. Buldyrev, A. L. Goldberger, S. Havlin, F. Sciortino, M. Simons and H. E. Stanley, *Nature* **356**, 168 (1992).
30. S. Roche, D. Bicout, E. Macia and E. Kats, *Phys. Rev. Lett.* **91**, 228101 (2003).
31. S. Lotfallahzadeh, M. Anvari, N. Ekhtiary, A. Esmailpour and M. R. R. Tabar, *Waves Random Complex Media* **25**, 9 (2014).
32. E. Fratini and S. Pilati, *Phys. Rev. A* **92**, 63621 (2015).
33. F. Battista, A. Camjayi and L. Arrachea, *Phys. Rev. B* **96**, 45413 (2017).
34. O. Narayan, H. Mathur and R. Montgomery, *Phys. Rev. B* **103**, 144203 (2021).
35. M. Ezawa, *J. Phys. Soc. Jpn.* **90**, 104704 (2021).
36. E. Díaz, G. Herrera, S. Oyarzún and R. C. Munoz, *Sci. Rep.* **11**, 1 (2021).
37. A. Mafi and J. Ballato, *Front. Phys.* **681**, 9 (2021).
38. F. A. B. F. de Moura, L. P. Viana, M. L. Lyra, V. A. Malyshev and F. Domínguez-Adame, *Phys. Lett. A* **372**, 6694 (2008).
39. F. A. B. F. de Moura, M. D. Coutinho-Filho, E. P. Raposo and M. L. Lyra, *Europhys. Lett.* **66**, 585 (2004).
40. F. A. B. F. de Moura, M. L. Lyra, F. Domínguez-Adame and V. A. Malyshev, *J. Phys., Condens. Matter* **19**, 56204 (2007).
41. F. A. B. F. de Moura, *Int. J. Mod. Phys. C* **22**, 63 (2011).